Noname manuscript No.
(will be inserted by the editor)

Non-linear Electrical Conductivity through the Thickness Direction of Multi-directional Carbon Fiber Composites

Xi Chen · Alexander Smorgonskiy · Jianfang Li · Anastasios P. Vassilopoulos · Marcos Rubinstein · Farhad Rachidi

Received: date / Accepted: date

Abstract Lightning strikes pose a serious natural threat to carbon fiber reinforced polymers (CFRP). Knowledge of the electrical current distribution is essential for modeling the interaction between CFRP with lightning. In most applications, the anisotropy of CFRP makes the electrical current tend to concentrate on the surface, having significant influence on the current distribution. The conductivity through the thickness direction was studied with pulse generators and a dedicated 4-probe fixture. Non-linear effects were observed not only for 6.4/69 μs lightning pulses, but also for 20/500 ns pulses with much less energy, in all the three tested composites. The electrical breakdown is a fast process, with voltage spikes observed in the leading edge for a few nanoseconds. After the spikes, the transient resistance remains approximately constant. Similarities could be found with the phenomena involved in thin polymer film breakdowns.

Xi Chen
Beijing Institute of Astronautical System Engineering, Beijing, China
Tel.: +86-10-88521724
Fax: +86-10-88382026-9031
E-mail: cxmicrowave@126.com

Alexander Smorgonskiy
IICT, University of Applied Sciences Western Switzerland, Yverdon-les-Bains, Switzerland

Jianfang Li
Aerospace Research Institute of Materials & Processing Technology, Beijing, China

Anastasios P. Vassilopoulos
CCLAB, EPFL, Lausanne, Switzerland

Marcos Rubinstein
IICT, University of Applied Sciences Western Switzerland, Yverdon-les-Bains, Switzerland

Farhad Rachidi
EMC Laboratory, EPFL, Lausanne, Switzerland

Keywords Carbon fibers · Electrical properties · Anisotropy

1 Introduction

Carbon fiber reinforced polymers (CFRP) offer great advantages over conventional materials, mainly due to their high specific strength and stiffness. However, lightning strikes pose a serious natural threat to high rise structures, such as wind turbines, as well as airplanes made of, or containing significant amount of composite materials [1, 2].

Modeling the lightning current interaction with CFRP is a challenging problem [3]. A good understanding of the CFRP material properties is the key to precise numerical models [1]. The electric conductivity, which has significant influence on the current distribution and also on power densities, has been investigated in numerous studies. The conductivity of polymers reinforced with electrically conductive particles can be estimated using microstructural data [4]. For composites with long fibers, theoretical models have been proposed based on equivalent electric conductivity tensors to calculate the piezoconductivity of composites [5], the resistance across the diameter of a rotating disc [6], or that of a sample with a given length and width [7]. Not only were the effects of fiber orientation [8] and thickness [9] taken into consideration, but also various experiments have been carried out to elucidate the validity of the equivalent electrical conductivity tensors [10]. Besides, a 3D resistor network model was formulated to predict the electrical conductivity of CFRP as a function of the electrical material properties and microstructural parameters such as fiber spacing and waviness [11]. As an anisotropic material, CFRP has higher conductivity along the fiber direction, but much lower conductivity through the thickness and transverse directions [11], which makes the electrical current tending to concentrate on the surface near the lightning attachment point, since CFRP blades are built in such a way that lightning generally strikes them perpendicular to the direction of the fibers.

A simple constant conductivity assumption might lead to extremely high Joule heating and unrealistic temperatures [1, 2]. Although the conductivity is assumed to depend on temperature in many models (e.g., [1, 2]), the dependence on the electric field is seldom considered. Nevertheless, simulations have shown that the potential at the lightning arc center position could reach several tens of kilovolts [1, 2] even when only 40 kA (1/5 of the amplitude specified by the standard [12]) is applied to CFRP plates with a thickness of a few millimeters. If the polymer thicknesses between plies are considered to be only a small fraction of the total thickness, the electric field may exceed 10^5 kVmm^{-1} through the thickness direction within the polymer, which is strong enough to cause discharges in most dielectrics. Generally, the term electrical breakdown is used when significant current flows through an electrical insulator, due to an applied voltage that exceeds the breakdown threshold. The term has been used in the context of CFRPs to describe similar significant increments in the electric conductivities [13], although they have higher conductivity than that

of insulators. If the electrical breakdown does occur, the conductivity increment might reduce the Joule heating significantly. Therefore, the non-linear electrical conductivity of multidirectional carbon fiber composites needs to be investigated, in order to model the lightning current interaction with CFRPs more precisely.

While several experiments have been performed to measure the electric conductivity under low current and room temperature [6, 7, 8, 9, 10], the number of investigations dealing with non-linear characteristics of CFRPs is limited [14]. Chekanov et al. [13] observed the breakdown effect of CFRPs with short cut fibers, which have much lower fiber content and also lower electric conductivity. The high voltage used was quasi-steady, with a duration around a second. Sun et al. [14] compared the dynamic impedance of several CFRP specimens with emphasis on the material surfaces. In fact, the conductivity through the thickness direction of long fiber reinforced polymers might exhibit non-linearity under high voltage as well, which requires detailed investigation. Besides, the transient response also needs to be analyzed, because the durations of lightning pulses are in the order of only a few tens of microseconds. The objective of this paper is to experimentally study the non-linear current-voltage behavior of CFRP samples through the thickness direction.

2 Experiment and procedure

Low resistivity, high current, high voltage and drastic heat dissipation pose challenges to the measurement of the non-linear electric conductivity of CFRPs. The first three points were addressed through the proper design of the test fixture, while the last was mitigated by using an impulse source. Small sample diameters were also used to increase the resistance through the thickness direction.

2.1 Samples

Fourteen CFRP specimens were fabricated for the purpose of this study. However, 6 samples were damaged in preliminary experiments, by conductive glues, surface discharges, etc., as shown in Fig. 1. The remaining 8 valid samples were cut from 3 different laminate plates listed in Table 1. All the 3 plates were off-the-shelf products, with different resins, stacking sequences and manufacturing processes.

Composite No. 1 was made from T300 carbon fibers [15] and E-14 epoxy [16], having a thickness of 2.7 mm, while composites No. 2 and 3 were made from T300 carbon fibers [15] and 610 flame retardant polymer [17], having a thickness of 2.1 mm. Fig. 2 presents schematically the stacking sequence of the composites. Composite No. 1 had a stacking sequence of $[+45/-45/0_2/90/+45/-45/0]_S$, with plain woven fiber cloths added at both the laminate surfaces. The temperature and pressure profile during the autoclave process is shown in

Fig. 3. Composite No. 2 was made with a stacking sequence $[(+45/-45)_2/+45/\overline{-45}]_S$, with plain woven fiber cloths placed on both the laminate surfaces as well. The temperature and pressure profile of the autoclave process is shown in Fig. 4. The last composite had a plain woven fiber cloth oriented in the $\pm 45°$ direction in the middle of the laminate, with two plies of $0°$ placed on both sides of the cloth. Twill woven fiber cloths were added to both the laminate surfaces. This composite was made with vacuum bagging at normal pressure using the same temperature profile of Fig. 4.

The profiles of all the 3 types of composites were investigated with microscopy as shown in Fig. 5. The dark regions in composites No. 2 and 3 were the phenol formaldehyde resin particles doped in the epoxy. Composite No. 1 contained the fewest polymer and the fibers were closely attached between the plies. In contrast, composites No. 2 and 3 had significant thick inter-laminar polymer. The resistances through the thickness direction measured with the low current 4-probe method are shown in Table 1. Composite No. 1 had the highest conductivity, while composites No. 2 and 3 had lower conductivity, which is caused by the different thicknesses of the inter-laminar polymers.

All the plates were cut by a milling machine to get round samples with a diameter of 11 mm, as shown in Fig. 6. All samples except sample No. 4 were polished before the experiment in order to measure the DC resistivity using low currents.

2.2 Test fixture

Although carbon fibers are not as conductive as metals, they are still good conductors. After electrical breakdown, the resistance of specimens might drop to a low value, sometimes even below 1 Ω. Therefore, the 4-probe method [18] is required to precisely measure the resistance which otherwise could be easily overwhelmed by the resistance of contacts and wires, as in our preliminary measurements. A robust connection between the electrode and the specimen is also necessary to sustain the high current. Conductive paste was used to establish the contact between electrodes and specimens during preliminary experiments. The paste had a conductivity of over 10^6 Sm^{-1}, and could provide a minimum bonding strength of 0.1 MPa below 155°C. However, it failed just after the inception of a electrical breakdown. Moreover, as mentioned earlier, CFRPs are anisotropic materials and, therefore, the conductivity in the fiber direction is much larger than that through the thickness direction, which makes the potential at the edges almost the same as the contacting driving electrodes on the same surface, even if the specimen has a diameter several times larger than the electrode dimension. This means that the voltage applied to the samples is also applied to the side surface. As a result, a CFRP/air surface discharge may occur prior to specimen electrical breakdowns. Therefore, a specifically designed fixture was fabricated to overcome these challenges, as described in the following paragraphs.

A schematic representation and a photo of the fixture are shown in Fig. 7 and Fig. 8, respectively. The specimen was clamped between the 2 brass tubes, which formed the 2 driving probes. Inside each tube, there was a brass pin isolated by PA6 nylon, which was the sensing probe. The brass tube, the nylon insulator, and the brass pin, formed a coaxial structure. Because the conductivity along the fiber direction was several orders of magnitude larger than that through the thickness direction, the potential between the driving probe and the sensing probe on the same side were almost the same. The 2 coaxial structures were mounted with screws on 2 stainless steel plates respectively. The top and bottom halves were insulated by 3 black polyformaldehyde plastic pillars.

The screws were placed on the inner surface of the plates, inner and outer surface of the tubes and nylon isolators, and also the outer surface of the pins. By turning the tubes while fixing the plates, pressure could be applied to the specimen in order to robustly attach the driving probes to the specimens. By turning the insulators with respect to the tubes, and the pins with respect to the insulators, the gaps between the insulators, pins and the specimen could also be minimized. Before impulse testing, the specimens were inserted into the fixture to measure the DC resistance. Tightening torques of 1 Nm and 1.5 Nm were applied to the brass tubes successively, with less than 1% differences of resistance observed, which implied that torques larger than 1 Nm were required for achieving a good contact.

The whole fixture was immersed in rapeseed oil to prevent surface discharges on the side walls of specimens. To verify this configuration, one of the specimens was further wrapped with EVA which has higher dielectric strength as shown in Fig. 9, but no significant difference in the results was observed.

2.3 Impulse sources

The power dissipation in the CFRP would heat the specimen drastically, which would make it almost impossible to measure the non-linear characteristic with constant current. Therefore, pulse sources were incorporated to prevent drastic temperature increments and polymer decompositions in the whole specimen.

The used impulse sources and the waveform characteristics are presented in Table 2. A 3CTEST LSS160SS source was used to generate the lightning waveform 1 of aircraft lightning standard SAE ARP 5412 [12], while a Montena EMP80K-5-500 source was used to generate conductive high altitude electromagnetic pulses (HEMP) conforming to the standard MIL-STD-188-125-2 [19]. Pulses were directly applied on the 2 driving electrodes (the brass tubes) of the specimens, with their currents monitored by a BCP-619 probe. Voltages were measured from the 2 measuring electrodes (brass pins) with a 100-MHz 6-kV high voltage differential probe. The diagram of the circuit is shown in Fig. 10. To mitigate electromagnetic interferences, the cables of the voltage measurement probe were arranged as close as possible and shielded as shown in Fig. 11.

3 Results and discussion

The tested samples are listed in Table 3. For each type of composite, two samples were tested with a standard lightning 6.4/69 μs pulse and a 20/500 ns pulse respectively, in order to investigate the electrical breakdown caused by standard lightning pulses and sub-mirosecond fast pulses. For the composite made from T300 fibers and E-14 epoxies, two additional samples were tested. One was tested after having been wrapped with ethylene-vinyl acetate copolymer (EVA), to make certain that the electrical breakdown did happen within the specimen, while the other sample was not polished, so that the damage to the surface resin could be observed with scanning electron microscopy (SEM).

During the test, the short-circuit current setting of the pulse source was increased by 3 dB per test step, that is, $\sqrt{2}$ times of the previous step. For example, if the short-circuit current was 100 A in the current step, it would be raised to approximately 141 A in the next step. Due to the finite source resistance shown in Table 2, the actual monitored current increment per step was a little larger than 3 dB. Each specimen only experienced 1 test cycle. After the current was increased step by step to the maximum and then decreased back to the initial value, the specimen was replaced to avoid severe cumulative damages. No obvious surface damages were visually observed during the whole experiment.

Standard 6.4/69 μs lightning pulses were applied to sample No. 1, 5 and 7. The typical current and voltage waveforms on sample No. 1 are shown in Fig. 12 (short-circuit output set to 1600 A). The current waveforms were characterized by expected double exponential shapes, while some voltage distortion could be observed in the first few microseconds. The waveforms of other samples were similar.

The plot of the peak voltage versus peak current is shown in Fig. 13. The arrows in the figure represent the sequence of test steps. All the curves have a similar shape. The V-I curves have an initial linear high increase rate, becoming significantly less steep after reaching a certain voltage, showing a non-linear effect. The voltage varied for different composites. It was lower for the sample made of E-14 polymer (for sample No. 1, approx. 470V), but higher for that made of 610 polymers (for sample No. 5, approx. 680 V and for sample No. 7, approx. 736 V). The thicker inter-laminar polymers might contribute to the difference. The V-I curve went back almost to the origin of plot for the composites made with autoclave technology (for samples No. 1 and No. 5), but intercepted the voltage axis at approximately 200 V for the sample made with vacuum bagging, which might be caused by the existing small defects of sample No. 7 as discussed in the following paragraphs. The DC resistance was measured after each pulse, as shown in the same figure. Compared to its initial value, the resistance dropped significantly after the electrical breakdown. Because the current of a lightning strike is fixed due to the high impedance of the plasma channel [20], the decrement of the resistance means much less energy (several orders of magnitude) is transferred into the material during the electrical breakdown. This result revealed that the assumption of a constant

resistivity in numerical simulations, as often adopted in the literature (e.g., [1, 2]), was not appropriate. It could also be observed that the resistance of the composite made at normal pressure exihibited more fluctuation.

For the HEMP 20/500 ns pulse, the typical waveform with a peak current of 660 A is shown in Fig. 14 (sample No. 2). The voltage waveform was characterized by a significant number of spikes in its leading edge, and an exponential shape later on. The waveforms of the other samples (No. 6 and 8) were similar.

One of the samples (No. 4) was observed with microscopy to investigate the damage caused by the HEMP 20/500 ns pulse with a peak current of 100 A. The surface of the specimen was not polished before the experiment, since polishing would lead to a number of small pits on the surface, which would hinder locating the pulse damage. The whole surface of the sample was photographed by regions before applying the pulses. It was then checked carefully after the experiment by comparing with the photos, to make certain that the defect was caused by the pulse. The 100X optical microscopy image is shown in Fig. 15. The red rectangular region in the photo is further magnified with SEM, as shown in Fig. 16. The epoxy was transparent to visible light but opaque to electrons. The pit of epoxy decomposition had a diameter of around 80 μm. It could be inferred that the current was not uniformly distributed, but concentrated in a few conductive channels. The dissipated energy within the specimen, integrated according to the Joules law [2] from the voltage and current waveform recorded by the oscilloscope, was found to be only a few mJ. However, irrecoverable resin decomposition still occurred even when the pulse energy was low.

To quantitatively evaluate the voltage-current (V-I) relationship, voltage values were extracted from the peak of the exponential fittings of the voltage waveforms, neglecting the voltage spikes. Fig. 17 shows the peak voltage versus peak current, where non-linear behavior can be observed as well with higher turning point voltage compared to Fig. 13. The arrows in the figure represent the sequence of test steps. The HEMP pulses were so short that their pulse widths were only 0.7 % of the 69 microseconds lightning waveform 1. Although the time duration varied by more than two decades, the turning point voltage was in the same order of magnitude. This showed that electrical breakdowns related weakly to the transferred energy but more to the applied voltage or electric field. The low current resistances of the samples went down after pulses, except that the resistance variation of the sample made with vacuum bagging showed irregularity. The fiber ablations caused by air discharges near the voids which were caused by low fabrication pressure might have led to the observed difference.

The electrical breakdown was a fast process. Significant voltage spikes existed in the leading edge, as shown in Fig. 14. The spikes could not be measured precisely, since they were so narrow that they exceeded the 100 MHz probe bandwidth. Moreover, the over-range audible alert of the probe sounded during the experiment, indicating that the actual voltage spike may have even approached 6 kV (the upper limit of the probe). These spikes were not due

to electromagnetic interference, since only small voltage spikes were observed in the comparative measurement where a low current was applied as shown in Fig. 18. Electromagnetic coupling was linear, which could not change the shape of voltage curves. The transient resistance (the ratio of voltage to current of Fig. 14 at every time point) remained almost constant after the spike (Fig. 19). Therefore, it seemed that conductive channels formed just within the spikes, in no more than a few nanoseconds. After that, the channels provided good conductivity. The resistance measured from the waveform was lower than that measured with DC after the pulse was applied, which might be attributed to the high temperature or discharge in of the channel during the pulse. In Fig. 12, no spike was observed since the rising edge of the lightning pulse was too slow. Electrical breakdowns happened repeatedly during the rising edge.

The above-mentioned electrical breakdown process looked similar to the breakdown of thin polymer films [21]. The formation of breakdown channels took place within a short period of nanoseconds. These channels kept their conductivity during the rest of the pulse, and they could be irrecoverable, therefore, still presented after the pulse was over. The breakdown field strength tended to grow slightly as the voltage rise rate increased. Assuming that the thin polymer film electrical breakdown theory [21] can be applied to the electrical breakdown of CFRP, the process would be described as folllows. Upon applying the voltage, the electric field between the plies drived electrons into the polymer. Tunneling takes place where the electric field strength was higher than its average value, especially where the fiber density was higher between plies. The electrons were captured by traps and formed space charges. As the space charges propagated toward the anode, the electric field near the ply with higher potential would increase. The current amplification initiating local destruction of the polymer was a consequence of the space charge evolution. The breakdown channel between plies was the outcome of the local Joule heating to high temperatures by an intense surge in the current (the formation of a hollow channel with conducting walls as a consequence of polymer decomposition and the formation of soot). It was believed that the electrical breakdown channels at the beginning could be as small as about 10 μm in diameter [21]. As the inter-ply polymers were broken down layer by layer, the voltage leading edge might comprise several narrow spikes. In addition, the defect within the composite would contribute to the electrical breakdown process. This could be observed from the samples made without the autoclave processes. The air discharge at the small voids could be recoverable, so that certain voltage was required by the air discharge and the I-V curve intercepted to a positive voltage.

4 Conclusions

An experiment setup using lightning and HEMP impulse generators with the 4-probe method to measure the CFRP resistivity through the thickness direction was presented in the paper. Three composites with different resins, stacking

sequences and manufacturing processes were tested. Non-linear effects were observed for all the samples. The conductivity through the thickness direction increased significantly when the voltage was high enough to cause polymer electrical breakdown.

Electrical breakdown was caused not only by 6.4/69 μs lightning pulses, but also by 20/500 ns HEMP pulses at a slightly higher voltage with much smaller pulse width and less energy, which suggested that the breakdown related weakly to the transferred energy but more to the applied voltage or electric field. By analyzing the waveform under HEMP, it was revealed that the electric breakdown was fast. Voltage spikes occurred in the leading edge during the first few nanoseconds. The transient resistance (the ratio of voltage to current at every time point) remained approximately constant after the spikes. These characteristics were found to be very similar to the electrical breakdown of thin polymer films. The tested composites were all off-the-shelf products. In further studies, composites could be intentionally fabricated with only one different parameter while keeping the others equal, in order to study the influence of resins, stacking sequences and manufacturing processes. All the measurements were performed with currents about 2 orders of magnitude below the lightning standards and the experiments were not intended to be destructive. Although information might be acquired for understanding the onset of the lightning interaction with CFRPs, attention should be paid while analyzing the period after high current and energy are applied, especially when gas from the decomposed resin and lightning plasma pressure might influence the resistance between plies.

The impedance through the thickness direction drops drastically after the electrical breakdown, and it should, therefore, not be regarded as constant. The relationship between the conductivity and the electric field should be taken into consideration in order to precisely model the damage of CFRPs stuck by lightning. Numerical models could be used in subsequent studies to better understand the involved mechanisms.

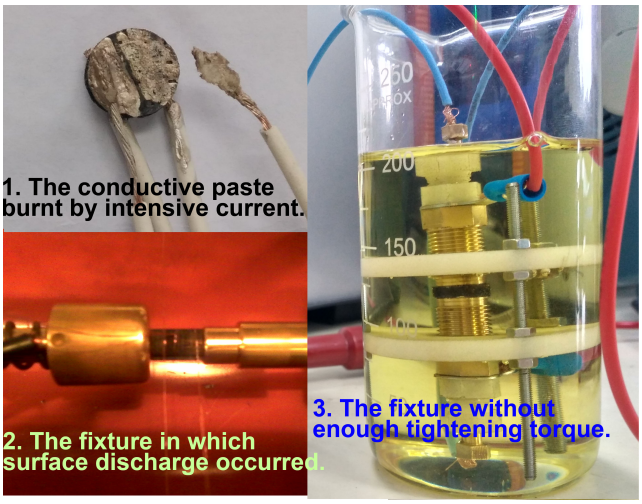

Fig. 1 CFRP samples damaged in preliminary experiments

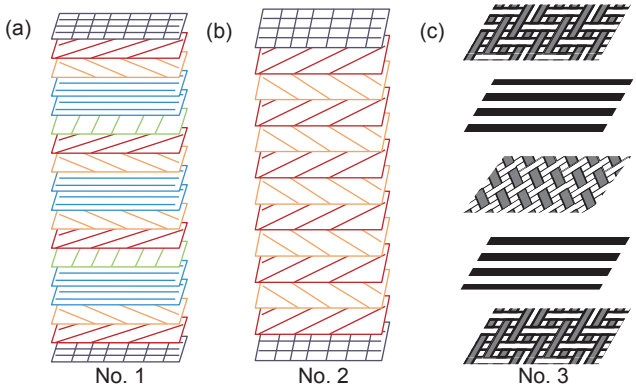

Fig. 2 A schematic of the stacking sequences

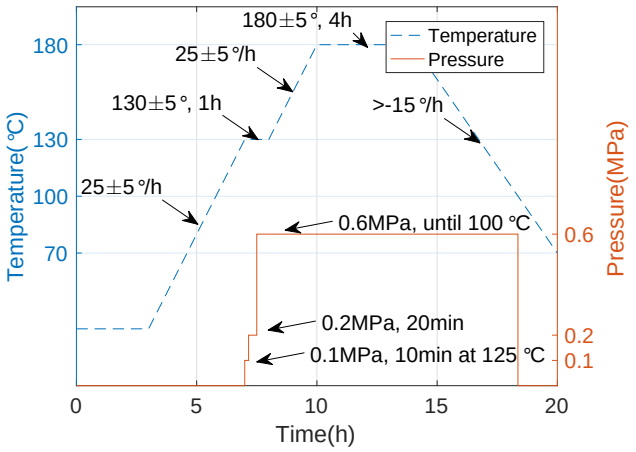

Fig. 3 The temperature and pressure profile during the manufacturing process of composite No. 1

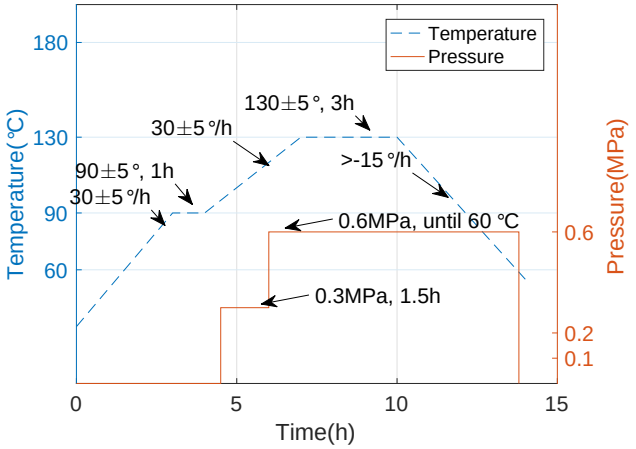

Fig. 4 The temperature and pressure profile during the manufacturing process of composite No. 2

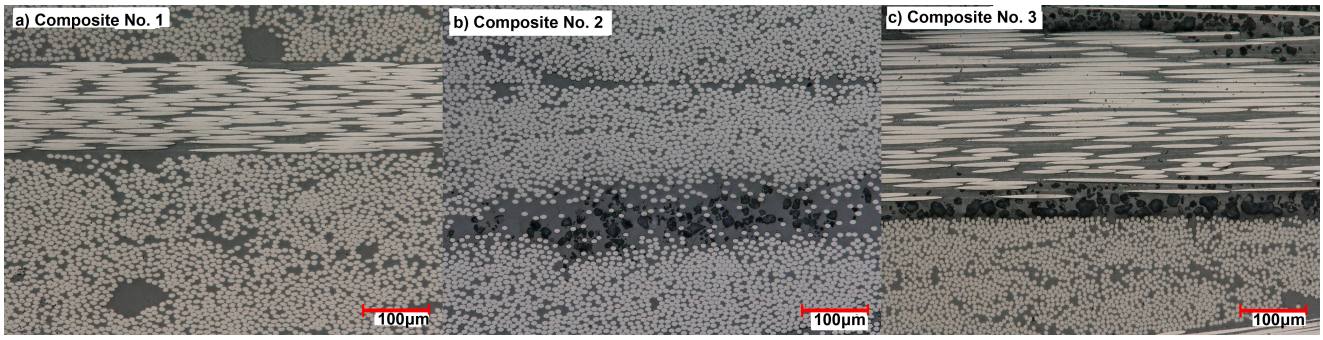

Fig. 5 The microscopy profile of the composites

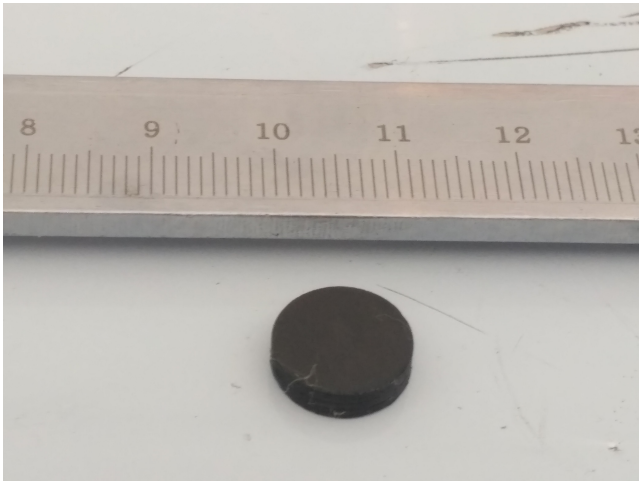

Fig. 6 The photo of a sample

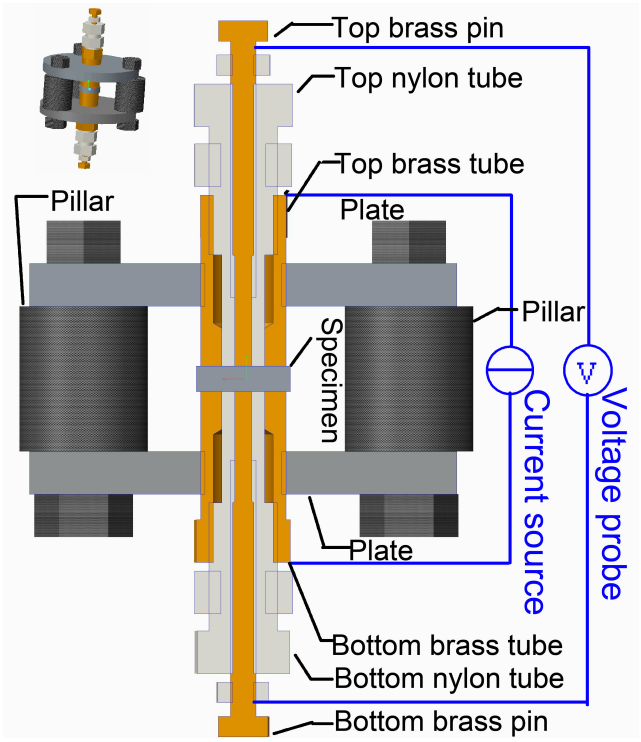

Fig. 7 The schematic representation of the test fixture

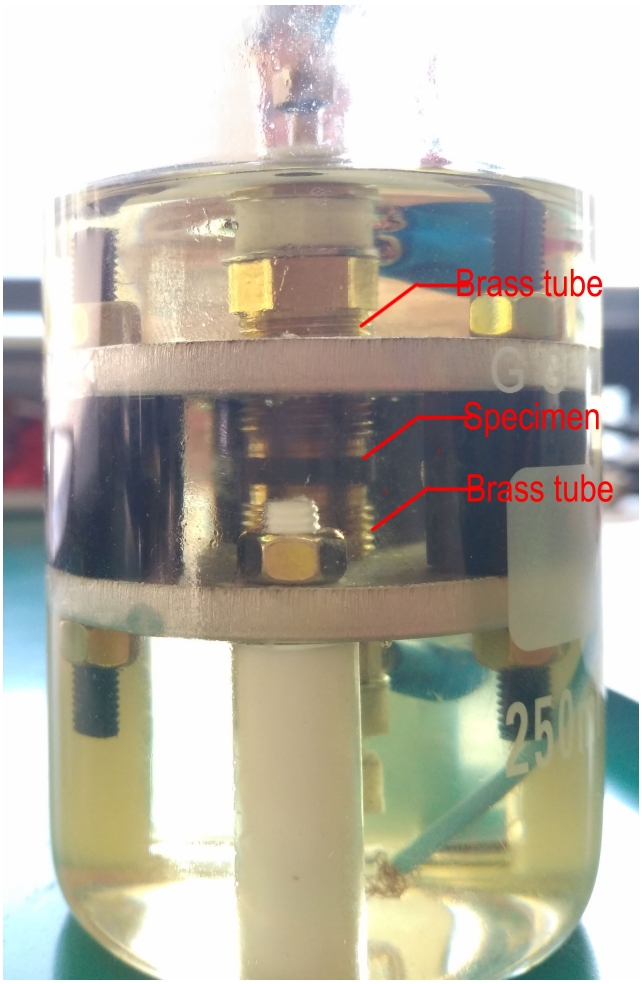

Fig. 8 The fixture with a specimen

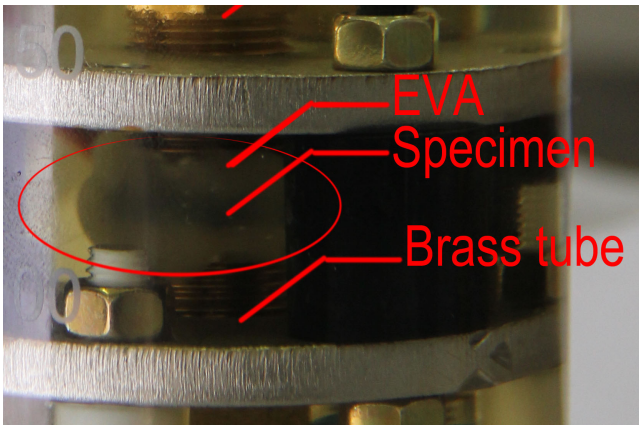

Fig. 9 The specimen wrapped with EVA

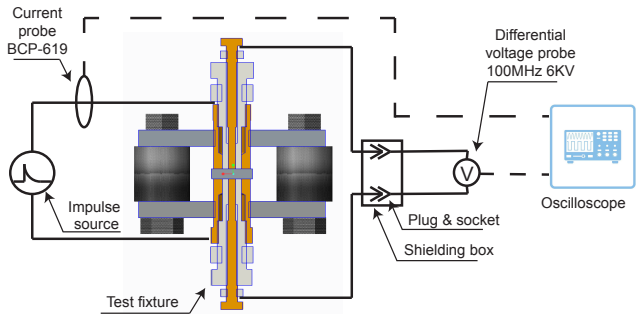

Fig. 10 The schematic representation of the experiment

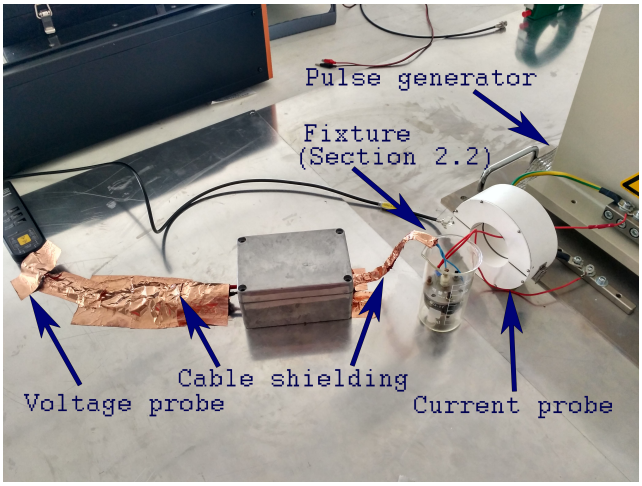

Fig. 11 The arrangement and shielding of cables

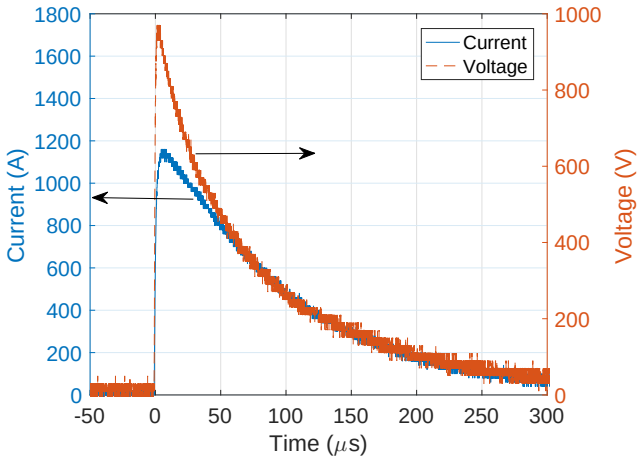

Fig. 12 Typical voltage and current waveforms under a 6.4/69 μs lightning pulse

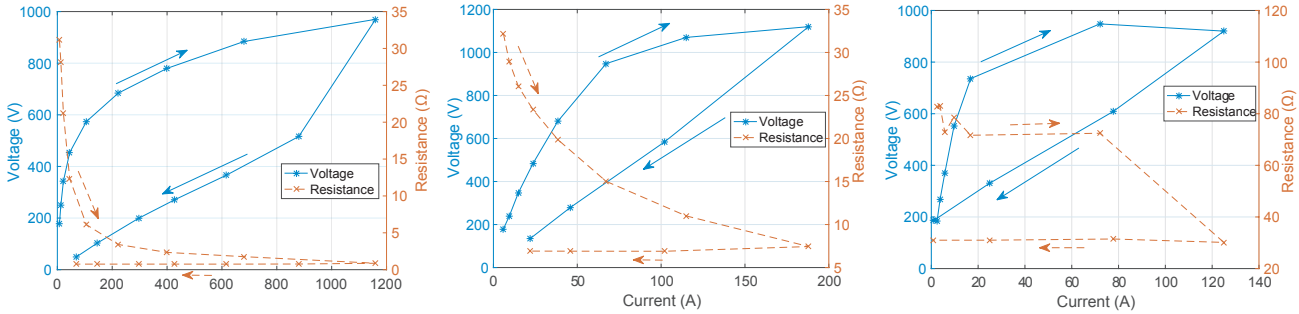

(a) Sample No. 1 (Composite 1) (b) Sample No. 5 (Composite 2) (c) Sample No. 7 (Composite 3)

Fig. 13 Peak voltage vs. peak current of the composites under 6.4/69 μs pulses

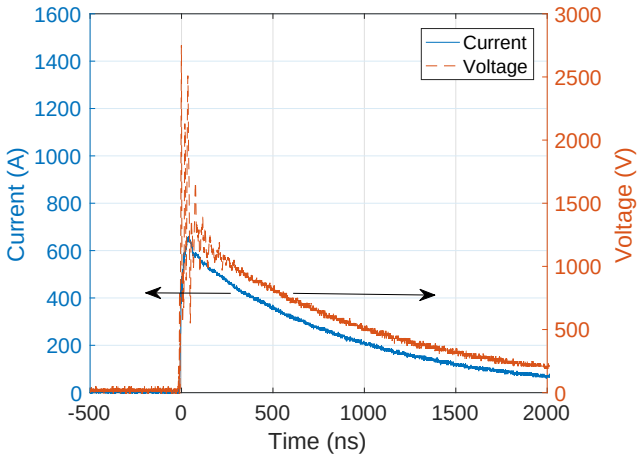

Fig. 14 Typical voltage and current waveforms under a 20/500 ns HEMP (660 A peak)

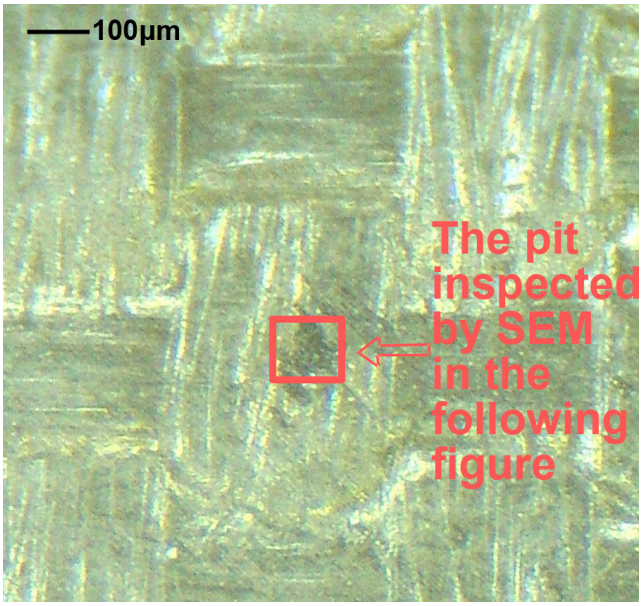

Fig. 15 The optical microscopy image of the sample surface

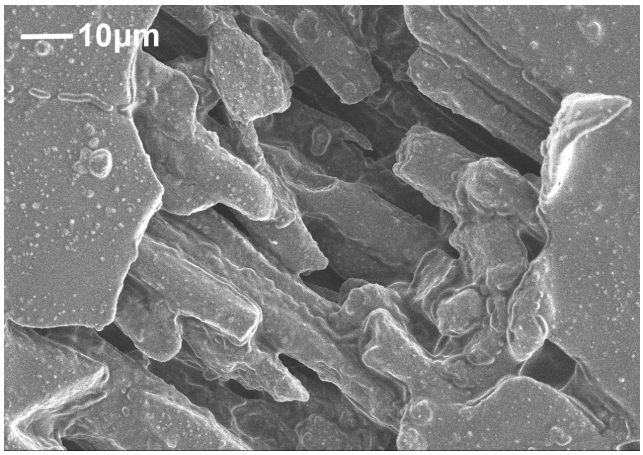

Fig. 16 The SEM image of the sample surface

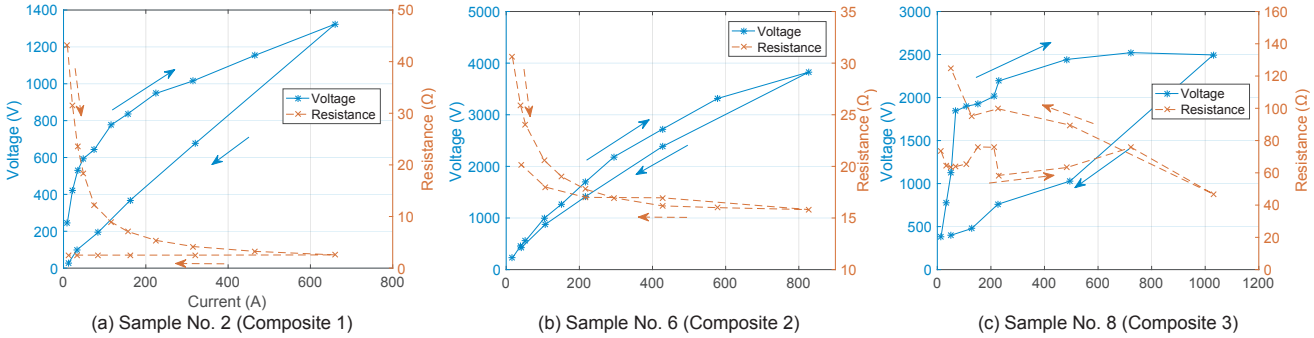

Fig. 17 Peak voltage vs. peak current of the composites under 20/500 ns pulses

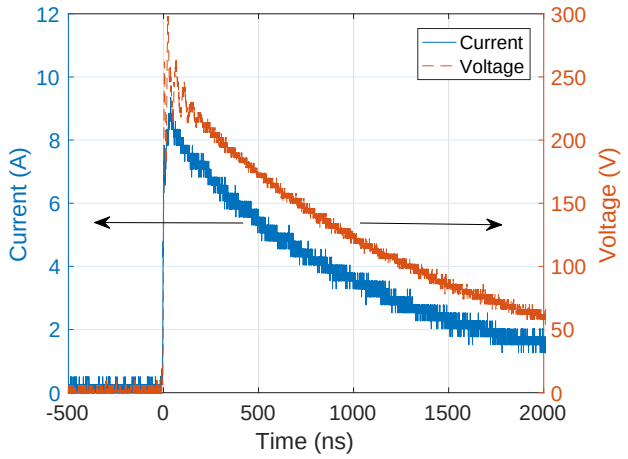

Fig. 18 Voltage and current waveforms of sample No. 2 under 20/500 ns HEMP (9.35 A peak)

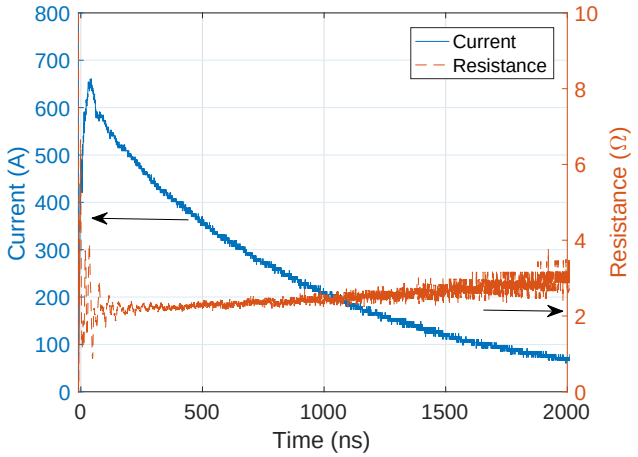

Fig. 19 The transient resistance of sample No. 2 CFRP sample (660 A peak)

Table 1 The tested composites

No.	Fiber	Resin	Manufacturing process	Temperature profile	Pressure profile	Thickness	Sample Numbers	Conductivity
1	T300	E-14	Autoclave	Fig. 3	Fig. 3	2.7 mm	1-4	0.919 Sm^{-1}
2	T300	610B	Autoclave	Fig. 4	Fig. 4	2.1 mm	5-6	0.334 Sm^{-1}
3	T300	610B	Vacuum bagging	Fig. 4	/	2.1 mm	7-8	0.213 Sm^{-1}

Table 2 Characteristics of impulse generators

	Waveform standard	Rise time	Pulse width	Generator	Source resistance
1	SAE-ARP-5412 Waveform 1	6.4 μs	69 μs	3CTEST LSS160SS	1 Ω
2	MIL-STD-188-125-2	20 ns	500 ns	Montena EMP80K-5-500	60 Ω

Table 3 The tested samples

No.	Composite No. referred to Table 1	Polished	Wrapped with EVA	Pulse
1	1	Yes	No	6.4/69 μs
2	1	Yes	No	20/500 ns
3	1	Yes	Yes	6.4/69 μs
4	1	No	No	6.4/69 μs
5	2	Yes	No	6.4/69 μs
6	2	Yes	No	20/500 ns
7	3	Yes	No	6.4/69 μs
8	3	Yes	No	20/500 ns

Compliance with Ethical Standards

Funding: This work was supported in part by the Swiss National Science Foundation under Project IZLRZ2-163907/1.

Conflicts of interest: The authors declare that they have no conflict of interest.

References

1. Abdelal G, Murphy A (2014) Nonlinear numerical modelling of lightning strike effect on composite panels with temperature dependent material properties. Composite Structures 109:268–278
2. Ogasawara T, Hirano Y, Yoshimura A (2010) Coupled thermal–electrical analysis for carbon fiber/epoxy composites exposed to simulated lightning current. Composites Part A: Applied Science and Manufacturing 41(8):973–981
3. Smorgonskiy A, Rachidi F, Rubinstein M (2014) Modeling lightning current distribution in conductive elements of a wind turbine blade. In: Lightning Protection, pp 1415–1417
4. Weber M, Kamal MR (2010) Estimation of the volume resistivity of electrically conductive composites. Polymer Composites 18(6):711–725
5. Xiao J, Li Y, Fan WX (1999) A laminate theory of piezoresistance for composite laminates. Composscitech 59(9):1369–1373
6. Greenwood JH, Lebeda S, Bernasconi J (1975) The anisotropic electrical resistivity of a carbon fibre reinforced plastic disc and its use as a transducer. Journal of Physics E Scientific Instruments 8(5):369–370
7. Tse KW, Moyer CA, Arajs S (1981) Electrical conductivity of graphite fiber-epoxy resin composites. Materials Science & Engineering 49(1):41–46
8. Knibbs RH, Morris JB (1974) The effects of fibre orientation on the physical properties of composites. Composites 5(5):209–218
9. AIAA (2012) Electric current analysis for thick laminated cfrp composites. Transactions of the Japan Society for Aeronautical & Space Sciences 55(3):183–190
10. Athanasopoulos N, Kostopoulos V (2014) A comprehensive study on the equivalent electrical conductivity tensor validity for thin multidirectional carbon fibre reinforced plastics. Composites Part B 67(67):244–255
11. Yu H, Heider D, Advani S (2015) A 3d microstructure based resistor network model for the electrical resistivity of unidirectional carbon composites. Composite Structures 134:740–749
12. SAE ARP 5412B (2013) Aircraft Lightning Environment and Related Test Waveforms. Standard SAE ARP 5412B, SAE International
13. Chekanov Y, Ohnogi R, Asai S, Sumita M (1999) Electrical properties of epoxy resin filled with carbon fibers. Journal of Materials Science 34(22):5589–5592

14. Jinru SA, Xueling YB, Wenjun XC, Jingliang CD (2018) Dynamic characteristics of carbon fiber reinforced polymer under nondestructive lightning current. Polymer Composites 39(5):1514–1521
15. (visited on 18.05.2018) T300 data sheet. URL http://www.fibermaxcomposites.com/shop/datasheets/T300.pdf
16. (visited on 18.05.2018) Epoxy resin e-14(603) datasheet. URL http://www.chem-shanfu.com/en/show/?id=1097
17. Cheng L, Ling H, Sun H (2012) Properties of 610 flame retardant epoxy and composite. Aerospace Materials and Technology 42(5):47–50
18. Yamane T, Todoroki A, Fujita H, Kawashima A, Sekine N (2016) Electric current distribution of carbon fiber reinforced polymer beam: analysis and experimental measurements. Advanced Composite Materials 25(6):497–513
19. MIL-STD-188-125-2 (1999) High-Altitude Electromagnetic Pulse (HEMP) Protection for Ground-Based C4I Facilities Performing Critical, Time-Urgent Missions - Part 2 - Transportable Systems. Standard MIL-STD-188-125-2, Department of defense
20. Chemartin L, Lalande P, Montreuil E, Delalondre C, Cheron BG, Lago F (2009) Three dimensional simulation of a dc free burning arc. application to lightning physics. Atmospheric Research 91:371–380
21. Zakrevskii VA, Sudar NT (2005) Electrical breakdown of thin polymer films. Physics of the Solid State 47(5):961–967